Numerical Analysis of an Innovative Blast Protective System for Buildings

Luís Miguel Marinho Pires
luismpires@tecnico.ulisboa.pt
Instituto Superior Técnico, Lisboa, Portugal
Academia Militar, Lisboa, Portugal

November 2021

Abstract

One of the fundamental principles that must be satisfied, is the safety and protection of human life, which occasionally is threatened by explosions derived from accidents or intentional actions. Studying an innovative protective system for infrastructures against explosions can help mitigate this threat.

Within the scope of TCor. Gabriel Gomes doctoral thesis (in progress) an innovative protective system was developed and successfully tested with proven capabilities. The present work, aims to contribute to this study by developing an advanced numerical analysis of this solution. Here the physical system is idealized into a 3D model using SolidWorks. Then the model is divided into elements using HyperMesh. Following the definition of the problem parameters through LS-Prepost, the input is processed by the solver LS-DYNA, and results are reviewed. Additionally, three methods are used to enhance the trust, efficiency and precision of results. Through benchmarking, mesh convergence and experimentation, the numerical study aims to comprehend and simulate the system behavior. On top of that, using simulation method, the numerical study aims to explore further ideas and solutions.

Findings reveal that the capacity of the system is high, reducing significantly the blast effects. Even when the system has imperfections, leading to eccentricities, it does not lose its performance, on the contrary it tends to improve. In the more severe cases, buckling phenomena may occur, but even then, the system always shows deformation by inversion, supporting the effectiveness of this absorption system.

Keywords: Blast; inverted tube; energy-absorption; LS-DYNA; numerical analysis.

1. Introduction

Explosives due to its intrinsic characteristics, its development has been illuminated by the intersection between military necessity and technological adaptation in the face of economic constraints [1]. This is the duality of all explosives; they are capable of many benefits, but they can also be chaotic and deadly.

Many of these events are associated to terrorism, which true cost goes far beyond the casualties and the financial loss. Media indirectly can play into terrorist organization's hands and aid them in their campaign of recruitment [2].

Europe seems to gain increasing interest in the use of explosives, especially improvised explosive devices (IED). Some are very easy to manufacture, remaining the most preferred, the homemade explosives, whose knowledge can be facilitated online. Considering the increasing risk of such events around the world, it is imperative to deal with this issue [3, 4].

1.1. Objectives and Methodology

A number of impact engineering problems have been investigated during the last decades, especially in the field of the dynamic response of structures in the plastic range. The research project PROTEDES (Protection of Strategic Buildings Against Explosions), where the doctoral thesis of TCor. Gabriel Gomes is included, aims to employ tubes, while focusing on the protection of infrastructures. Nevertheless, one of the most interesting variations, the tube inversion, is adopted. A major limitation of this structure is the lack of reliable information on its deformation mode regarding the dynamic behavior, mainly because most of the existing studies were performed under quasi-static conditions.

The present dissertation aims to contribute to deepen the knowledge of the phenomena, with the following major objectives:

- To present the experimental activity, explaining the mechanism of energy absorption device, its

respective testing campaign and results;
- To build a highly-detailed 3D model of both the energy-absorption device and the entire protective system;
- To perform a numerical analysis with a strong focus on simulating the true dynamic behavior of the protective system against blast effects based on experimental test data provided by Gomes' doctoral thesis;
- To contribute to the development of knowledge in this area, particularly regarding this protection system, addressing: i) The analysis of the effect of magnitude of the blast wave and initial impact velocity; ii) The understanding of deformation modes, and their mechanisms; iii) The study the energy dissipation efficiency on the building's shield; iv) The determination of the maximum capacity of both of the connector alone and the whole system; v) The assessment of how the presence of the energy-absorption devices dynamics affects the performance of the system; vi) The evaluation of the influence of different scenarios and variables.

2. Theoretical Background

2.1. Introduction

The unpredictable and destructive aftermath posed by explosions can emerge from accidental hazards to intentional acts of mankind. Therefore, it has been established a concern and a need to consider the behavior of engineering structures under blast loading to enhance the capacity to predict the effects of an explosive blast for design proposes. When designing structural elements to resist blast loads, the most effective and least costly mitigation approach is to increase the standoff distance [5, 6]. If not possible, protective measures and systems should be used alone or combined, such as a) shielding a structural element; b) provide catching systems to allow existing elements to break, and c) protective hardening protective structural elements and connections, which is an option that can be essential to withstand gradual collapse [7, 8].

2.1.1 Explosions and Blast Effects

Explosions categories may be: physical, nuclear, or chemical events [9, 10, 11, 12]. Once chemical events are, to a great extent, the most common, the analysis will be focused on them. The explosion phenomenon can be defined as the combustion of explosive material, a very rapid chemical reaction, faster than the speed of sound, which makes a detonation, and produces transient air pressure waves, called blast waves. A huge amount of energy and hot gases is produced by an action that only lasts some milliseconds, decaying back to ambient pressure over a short duration of time [9, 13].

During detonation, the hot gases produced expand outwards by pushing the surrounding air through space, leading to the wave type propagation transmitted spherically and forming a small layer of highly compressed air on the wavefront, the shock wave. It contains a large part of the energy released during detonation and moves faster than the speed of sound [14]. As the shock wave travels moving away from the focus, the air around that region cools down and reduces the pressure.

2.1.2 Explosion Types

Explosions can be specified in function of their location relatively to the target and the degree of the confinement, which provides information and guidance on the construction of structures to withstand the effects of explosions. They can be classified as confined explosions, unconfined explosions or explosive attached to a structure. Non-contact, unconfined explosions, external to a structure will be the ones considered in this research. They can be subdivided into: free-air burst; airburst and surface burst [15, 16].

2.2. Surface burst

Surface burst is the type of explosion adopted, in the context of the experimental testing campaign, since it is the most common in terrorist attacks [41]. In such explosions, amplification occurs at the point of detonation due to the ground reflections. Hypothetically assuming that the ground is a rigid surface, the generated pressure would be twice that produced by the same charge under free-air burst conditions. However, as energy generated by the explosion is partially absorbed by the ground. Instead an enhancement factor of 1.7 to 1.8 is taken [15, 16].

2.3. Shock Wave Reflection

When a shock wave intersects a solid surface, as illustrated in Fig. 1, it becomes subjected to amplification and reflection phenomenon, being the reflected peak pressure (P_r) always higher than the incident pressure that originated it.

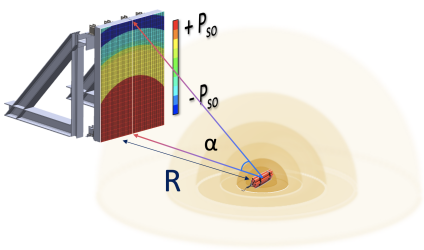

Figure 1: Numerical model representation of the reflected pressure on the simulated protective system. This image clearly shows two very important aspects: i) the influence of the impact angle on the magnitude of the reflected pressure, and ii) the fact that the shock wave propagates spherically.

Hypothetically, in an ideal linear-elastic case, the surface would experience approximately the double of the acting pressure. The value of the pressure reflected from the surface becomes maximum at the point of normal distance between the detonation source and the surface.

The reflected pressure's value decreases as the α (angle of incidence) increases and it can be determined by several methods. The most common being the Rankine and Hugoniot [9, 17]. Eq. 1 can be derived:

$$P_r\,[MPa] = 2P_{so} \cdot \left(\frac{7P_o + 4P_{so}}{7P_o + P_{so}}\right) \tag{1}$$

According to this equation the maximum and minimum values of the reflected pressure can vary from two to eight times the incident pressure. Nevertheless, experimental investigations have concluded that can be several times higher than eight times the incident pressure, due to the non-linear effects of the blast wave phenomenon ([15]). This equation is only valid in the case of normal reflection ([17].

2.4. Blast Wave Characterization

During the late 1950s-1980s, blast wave parameters of conventional HE materials have been widely investigated in several studies [16, 18, 19, 15]. All blast wave parameters are graphically sketched in UFC 3-340-02 [15], concerning the scaled distance using the test data collected by Kingery and Bulmash [19]. The most relevant are:

- P_{so} peak incident pressure, also known as side-on overpressure or peak overpressure;
- t_o^+ positive phase duration;
- i_s^+ positive impulse or specific side-on impulse associated with the positive overpressure phase;
- t_a arrival time of the blast front;
- P_r peak reflected pressure;
- i_r reflected impulse.

The idealized profile of pressure in relation to time for the case of a free-air blast wave, measured in an element at a certain distance, represented in Fig. 2, is described from the moment of detonation.

Initially, the pressure on the element is equal to the ambient pressure (P_o). It undergoes an immense increase of incident pressure, upon the arrival of the shock wave. After its peak value (P_{so}), the pressure decreases rapidly with an exponential rate until it reaches the ambient pressure, and becomes even lower (referred to as negative pressure), and finally returns to it. In this negative phase, the structures are subjected to suction forces.

The area under the pressure curve corresponds to the impulse caused by the detonation in the

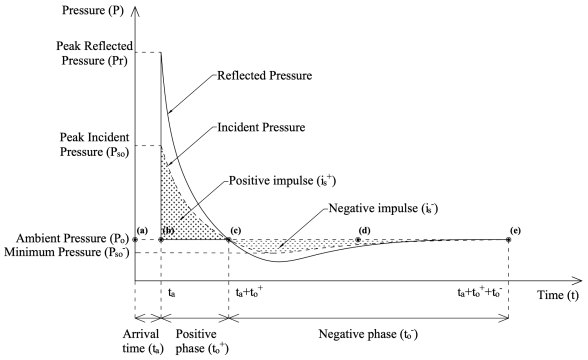

Figure 2: Typical air blast pressure profile on the left with respective illustration of its effects on the right, adapted from [9].

structure, being this parameter one of the most relevant in the case of external explosions to characterize the destruction mechanism.

The pressure drop through time is usually represented by the modified equation of Friedlander (Eq. 2) [16, 15]:

$$P_s(t) = P_{so} \cdot (1 - \frac{t}{t_o}) \cdot e^{-\beta \frac{t}{t_o}} \tag{2}$$

where $P_{so}\,[kPa]$ corresponds to peak incident pressure, $t_o\,[ms]$ to the duration of the positive phase, $t\,[ms]$ the period of time between the instant of arrival (t_a), and β is the decay coefficient of the curve.

For modeling purposes, in this research, the Friedlander fitting curve will be used, due to experimental data being available, which enabled the decay coefficient to be calculated through a non-linear fitting of an experimental pressure-time curve over its positive phase. The following Eq. 3 also constitutes a possible computing method, only when the values of the i_s, P_{so}, and t_o are known from experimental data by solving iteratively for the decay parameter β [16, 15]:

$$i_s\,[MPa \cdot ms] = \frac{P_{so \cdot t_o}}{\beta^2} \cdot \left[\beta - 1 + e^{-\beta}\right] \tag{3}$$

2.5. Scaling Laws

One of the most crucial parameters for blast loading calculations is the distance of the detonation point from the structure considered, the scaled distance in (Z). The effect of distance on blast characteristics can be taken into account by the introduction of scaling laws. The most ordinary blast scaling laws are the ones defined experimentally by Hopkinson-Cranz and Sachs, described by Eq. 4 [9, 16, 15]:

$$Z = \frac{R}{W^{\frac{1}{3}}} \tag{4}$$

2.6. TNT Equivalence

The term "TNT equivalence" is applied to measure the effects of the output of a given explosive by

comparing it to that of a TNT explosive [11]. More information is available about the properties of the blast waves produced by TNT than by any other explosive. In short, it gives us the relative strength of explosions [20].

3. Protective Solution and Experimental Results

3.1. Introduction

Current literature lacks reliable information on open sources regarding the dynamic behavior of energy absorption devices adopted against blast effects. This work is part of two ongoing complimentary projects, that are trying to develop high performance protective solutions against blast loading, namely BLADE[1] and PROTEDES[2].

The protective system developed and tested experimentally is based on a rigid panel (reinforced concrete) to which are connected a plurality of ductile metallic connectors, designed to explore an inversion mechanism.

The system has three main purposes. Firstly, rigid panels receive the blast directly, which reduces the reflected pressure and impulse directly imparted to the structure. On top of that, it offers protection from flying fragments, impact, and fire. Secondly, plastic deformation of the connectors, dissipates most part of the energy from the explosion, reducing the energy transmitted to the structure. Thirdly, the location of the connectors allows to simultaneously redirect the transferred energy to the slabs of the structure, protecting vulnerable elements (e.g., columns).

3.2. Energy-absorption connector

A number of problems have been investigated in the field of energy-absorption connectors. There are several typical energy absorption structures, being tubes one of those [21, 22]. A structure that starts to deform axially can suddenly buckle in the global bending mode, causing a significant drop in the structure's capacity to absorb the impact energy [23]. However, this issue was addressed by using one of the most interesting variations of this structure, the tube inversion, which has the most efficient energy deformation mode among the ones possible. It additionally enables a deformation with a constant inversion load.

3.3. Materials

3.3.1 Reinforced Concrete Slab

For this study, sixteen reinforced concrete panels were produced. Material properties were determined by Gomes [8], through tensile tests on steel and uniaxial compressive tests on concrete cylinders. Each panel had the characteristics presented in the following Tab. 1 to 3.

[1] Blast Protective Walls Design Optimization
[2] Protection of strategic Buildings Against Explosions

Table 1: Reinforced concrete slab characteristics [8].

Concrete	
Strength Class	C25/30
$f_{cm}[MPa]$	33
$f_{ctm}[MPa]$	2.6
Slab dimensions $[m]$	2.75 x 1.00 x 0.21
Concrete cover $[m]$	0.025

Table 2: Tensile characteristics of the steel tubes [24].

Specimen $[mm]$	E$[GPa]$	$\sigma_{y(0.2\%)}[MPa]$	$\sigma_u[MPa]$	$\varepsilon_{max}[\%]$
Φ 64 x 2	210.6	371	423	16

Table 3: Tensile characteristics of the steel rods [8].

Specimen $[mm]$	E$[GPa]$	$\sigma_{y(0.2\%)}[MPa]$	$\sigma_u[MPa]$	$\varepsilon_{max}[\%]$
Φ 16	200	542	639.3	5

3.3.2 Energy Absorption Device

In this study, three tube diameters were used (64 mm, 54 mm, and 42 mm) to better understand the inversion mechanism and check the importance of the different influencing parameters. Due to time constraints, the 64 x 2 [mm] was the diameter analyzed in the present research. Physical characteristics are presented in Tab. 4. On Fig. 3 and 4, it is possible to check the application of the tube on the connector, as well as the dynamics of its mechanism.

Table 4: Detailed characterization of the tube measurements [24].

Inverted tube 64 x 2 [mm] characteristics	
Nominal diameter $[mm]$	64
Tube thickness $[mm]$	2
Radius (r_o) $[mm]$	32
Plug lenght $[mm]$	30
Plug diameter $[mm]$	58
Inversion radius (r_{inv}) $[mm]$	12
Ratio (r_{inv}/r_o) $[mm]$	0.375
Max compressing force $[KN]$	121
Diameter expanded $[mm]$	90

Figure 3: Representation of a section cut from the Energy Absorption Device (EAD), within the protection system [8].

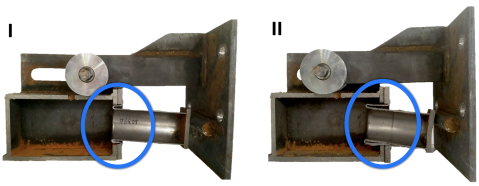

Figure 4: Cut section of the EAD. I) Before the blast. II) After the blast. Reproduced with the authorization of Gomes [8].

3.4. Components

The absorption connector includes several components, as shown in Fig. 5.

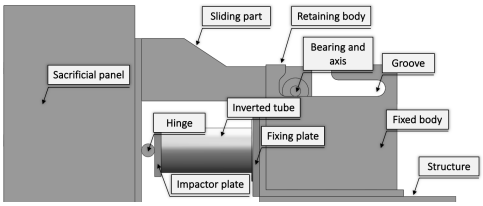

Figure 5: Capture of the different components that constitute the EAD.

3.5. Explosive

The explosive used in the associated experimental campaign is known by the name of "Goma-2 ECO", commercially sold as RIODIN by MAXAM's. Allegedly used in the March 11, 2004 train bombings in Madrid by the Al-Qaeda terrorist organization, is a Spanish-made high explosive intended primarily for industrial use, such as mining and demolition, or military applications. The blast test was conducted with an explosive load of 60 kg.

3.6. Blast test setup

The blast testing campaign is arranged radially comprising 4 metallic setups, allowing simultaneously testing as illustrated in Fig. **??**.The defined arrangement intends to make the explosion affect panels equally, being the distance between the panel and the explosive was 5.0 m.

3.7. Results data

3.7.1 Pressure

All tests were monitored with pressure gages, allowing tracking of the incident pressure, presented in Tab. 5 [8].

Table 5: Experimental data, with the average adjusted parameters for both sensors [8].

Sensor ID	P_{so} $[kPa]$	t_o $[ms]$	i_s $[kPa \cdot ms]$	α $[-]$
Ground	1256	1.9	526.82	3.12
Elevated (2.5 m)	765.7	1.9	410.05	1.34

3.7.2 Impact Angle, Shortening deformation and Force

Another interesting, although expected observation, is that the pressures measured by the elevated sensor were lower than the one on the ground, illustrated in Fig. 6. The reason for this effect is the impact angle, which, when it increases, values of pressure decrease.

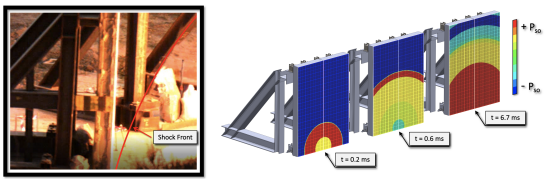

Figure 6: On the left, representation of the footage from high-speed cameras [8]. On the right, representation of pressure fringe plot across three-time intervals from the numerical analysis, to capture the influence of impact angle over time, across the slab length.

Additional data was collected, and in terms of deformation, an average total inversion length of 87 mm was considered later in the numerical analysis for the calibration and validation of the model. Force plots also clearly show the effect of introducing an EAD, in reducing the impulse transmit ed to the protected structure.

3.7.3 Observations

Additionally and according to the results obtained, it was observed relevant observations namely: i) a differential response at the bottom and top connectors; ii) in one case, part of the energy was absorbed by the bending mechanism and by pulling out the screws from the concrete base; iii) Buckling of the tube walls did not occur, even when significant rotation occurred, which represents promising performance in terms of effectiveness and reliability of the protective system; iv) In most cases, an eccentric impact occurred, causing a slight rotation of the EAC.

4. Development of Numerical Models

4.1. Introduction

Generally speaking, traditional methods, involve the idealization of physical models through simple equations to obtain solutions. Alternatively, finite element methods, and other numerical methods, are meant to provide an analysis that considers greater detail, leading to more precise and accurate results [25, 26].

The finite element method is an advanced technique used to solve complex structural analysis problems. It involves discretizing a geometry into finite elements, connected by nodes and used in a finite element solver to obtain approximate solutions [26]. Additionally, nonlinear finite element analysis techniques have been widely used to analyze structural elements, including reinforced concrete slabs under blast loads [27].

4.2. Methodology

The process started with the creation of the different individual bodies geometries that constitute the system. This task was conducted with SolidWorks® Academic Version 2020-2021.

Afterwards, Altair® HyperMesh® Version 2021 was employed as a pre-processor to mesh the geometric model, dividing it in thousands of polygonal shapes, each of them representing an element.

Subsequently, LS-Prepost was also used as a pre-processor to define the problem parameters. The analyses were then conducted through the solver LS-DYNA, achieving the problem's approximate solution. Following the analyses, the results were imported once again to LS-Prepost. In this step, the latter was used as a post-processor to convert the output into a readable or visual form.

Autodesk AutoCAD® 2018.2 Version O.48.M.563 was also used as a secondary tool, to develop part of the Load Segment method (LSS), read the protective system drawings and create figures.

To complete the analysis, a set of studies was performed afterwards to produce a more trustworthy numerical study. Furthermore, results, problems, and setbacks are presented, aiming at explaining the methods adopted and the decisions made.

4.3. Software

4.3.1 SolidWorks Modeling

The need for precision, such as considering all the eight critical tube characteristics, turned the modeling creation process into an unpractical and time-consuming task. Thus, considering the limitations and knowing that details would largely influence the quality of the outputs of the numerical analysis, it was necessary to define an adequate method, which led to SolidWorks, a Computer-Aided Design software.

When developing a SolidWorks design, all the components (parts) were designed, and put together (assembly), building the 3D model.

Some struggles were faced with major lessons learned. Among those, a relevant matter is the level of detail. It was a time-consuming mistake during the modelling process to craft the model geometry precisely as in reality. It relates to the idealization of the model. In the end, the goal is a simpler model, however, not at the cost of having bad results.

4.3.2 HyperMesh Meshing

Within HyperMesh, it was possible to mesh the 3D model created. The feature that helped most was the advanced automation tools, allowing mesh optimization from a set of quality criteria, such as the "Solid Map". Being further able to locally control the number of nodes to create compatible meshes with different and adaptive mesh densities.

4.3.3 LS-Prepost

The process with LS-Prepost embraces two separate actions. As a pre-processor, there are essential steps related to all the ongoing definitions and parameters incorporated in the LS-DYNA input file. As a post-processor, it is possible to explore and analyze results in several possibilities, such as visual animation, fringe plotting, data history plotting, among others.

4.3.4 LS-DYNA

LS-DYNA is the solver used, based on the FEM, initially called DYNA3D, which primary applications were to analyse bombs dropped by US Air Force Jets [28]. The specific attraction of this software to the industry started with its nonlinear dynamic capabilities.

4.4. Model Characterization

4.4.1 Material Calibration

Reinforced Concrete Slab Modeling

Concrete, a brittle material which resistance and damage behavior are strongly influenced by loading rate, is used in the slab of the protective system. Therefore any material model should incorporate these nonlinear characteristics. However, due to concrete characteristics, dynamic experiments that determine these parameters are much more complicated and expensive than the static load test [29, 30]. Consequently, responses predicted by numerical analyses have been important resources for academics and structural engineers to determine the behaviors of reinforced concrete structures submitted to dynamic loads [29, 30].

LS-DYNA Constitutive Concrete Models

LS-DYNA offers several constitutive material models to simulate the structural behavior of reinforced concrete [29, 30, 31]. In the context of blast and dynamic analysis, studies described it as a reliable model when compared to experimental values [30, 32, 33]. CSCM constitutive mode, known as Continuous Surface Cap Model, is a concrete material option developed in the United States of America for road safety. Sponsored by the department of transportation to predict the dynamic performance, both elastic deformation and concrete failure [29, 34]. Even though the model was developed and evaluated for roadside safety applications, it should also apply to many dynamic problems [34].

Reinforcement and Connector Modeling

The material models used for the steel parts were Plastic Kinematic (MAT003) and Rigid

(MAT020).

LS-DYNA Constitutive Plastic Kinematic Material

The Plastic Kinematic material model was formulated by Krieg and Key [35]. This material was applied in reinforcement, partly on the support structure of the connector and finally on the inverted cylinder. Consequently, the Cowper Symonds model Equation was used to take into account the strain-rate effect under blast loading, which scales the yield stress by a strain-rate dependent factor:

$$\sigma_y = DIF \cdot \sigma_o = \left[1 + \left(\frac{\dot{\varepsilon}}{C}\right)^{\frac{1}{P}}\right] \cdot \sigma_o \qquad (5)$$

Where DIF, Dynamic Increase Factor, is the strain-rate dependent factor, $\dot{\varepsilon}$ is the strain-rate, σ_o the initial yield stress, C and P are the strain-rate parameters for the Cowper-Symonds model [35].

LS-DYNA Constitutive Rigid Material

Parts defined with rigid material model, MAT_020, are considered to belong to a rigid body. In practice, RIGID parts do not increase the run time, only the file size.

4.4.2 Optimization and Simplification

Due to the high cost of this analysis, every effort was put in place to simplify and improve its cost-efficiency. Considering the model, geometry simplification was a possible through symmetry. Another simplification was the detonation time offset, which does not consider the time that the wave takes to arrive at the target. One similar simplification is the *DEFORMABLE_TO_RIGID keyword. Additionally, considering all the materials models available, the models chosen are cost-effective for both materials, reinforced concrete, and steel. As mentioned already, when possible RIGID materials were considered. Until now, solid elements have been used for the inverted cylinder. Instead, it was used shell elements. The change to shell elements saved a lot of computational solve time and improved numerical results.

Blast testing

The principle adopted during analysis was to reason from first principles and not only by analogy. With this approach, if a mistake happened, it would be easier to identify. Therefore, every study was done isolated, at the start.

4.4.3 Element Types

Every element is made up of nodes, which connect the ends of the elements. Defining the elements can be done in different ways, namely section-wise with solid, shell, and beam elements. Beyond solid elements, beam and shell elements also play an important role in numerical analysis. For many applications, far too many solid elements would be needed to obtain a decent solution because solid elements must have a reasonable aspect ratio to be accurate. They are commonly used to simplify and speed up the analysis whenever they are adequate.

4.4.4 Contacts and Constrains

LS-DYNA has hundreds of different contacts, and it is necessary to define them. They are important to avoid errors, elements penetrations, and even unreliable results (e.g., negative volume elements). In the model nodal rigid body constrains were defined for each EAD, to attach it to the wall.

4.4.5 Deformation Control

Using hexahedral elements has its advantages, mostly the combination of accuracy and runtime efficiency. Their employment usually becomes more economical than other solid element formulations. However, there are some possible modes of deformation, such as locking and as hourglass that must be considered.

4.4.6 Output Database

The output files which contain the results information are defined previously in the database keyword group. It can be done in several formats and options. The options used were: ASCII: mainly used for hourglass and energy (GLSTAT and MATSUM), on top of that it was used for the force results (RCFORC); D3PLOT and D3THDT for aditional data (stresses, strains, energy, velocities, among others).

4.4.7 Termination Time

In LS-DYNA, the analysis is stopped at a specified time, called the termination time, which is determined by the keyword *CONTROL TERMINATION. Additionally, it needs to be precisely defined to be cost-effective and long enough to capture all the pretended information avoiding delaying the analysis and wasting processing resources. Between all the models, this value ranged between 0.009 seconds to 0.1 seconds.

4.4.8 Mesh Quality

A simple mesh with good quality elements or a refined mesh with bad quality elements can create a slower analysis than expected. Additionally it tends to create distortion of the elements. According to

Fig. 7 example, I) shows a simple mesh which runtime was high (up to 22 days) and gave bad results (error $\approx$ 13 %), while both II) and III) are good models, which are fast (less than 3 hours) and produced accurate results (error $\approx$ 2 %), being the last one more refined.

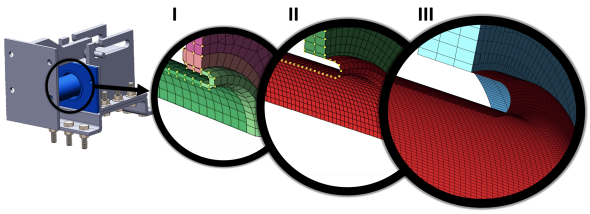

Figure 7: Representation of three examples of mesh improvement.

4.4.9 Strain-Rate Effects

This is a highly dynamic problem. Thus, it is important to consider the strain-rate effects. In the steel material chosen (MAT_003), those effects are considered when defining the constitutive materials through Cowper-Symonds parameters. These parameters have been widely studied, and there are several contributions in the available literature, as can be seen in Tab. 6.

Table 6: Cowper-Symonds parameters for mild steel.

Publication	C	P
Cowper & Symonds [36]	40.4	5
Abramowicz & Jones [37]	6844	3.91
Abramowicz & Jones [38]	802	3.585
Yu & Jones [39]	1.05E7	8.3
Marais et al. [40]	844	2.207
Jama et al. [41]	844	2.207
Sun & Packer [42]	3023	1.65

4.4.10 Blast Load Alternative Methods

Initial Velocity Generation (IVG) is an alternative method that imposes an initial velocity on the selected elements. It is a cost-effective method to create the desired deformation, similar to the one created by the blast, seen in the experimental campaign tests, was used initially to model the deformation behavior.

Load Segment Set (LSS), the alternative, more appropriate method, and cost-effective. Was possible to use, due to having the experimental curves. Since this method applies blast pressure data, it does not consider the angle of incidence on the wall, nor the spherical shock wave propagation (Fig. 8). This effect along the span length is not considered with this method, and it plays a remarkable influence on the system's behavior.

In the end, both methods velocities results were volatile , and the minimal fluctuation could produce significant deviations that made it impossible to calibrate the model under the recommended 10% error.

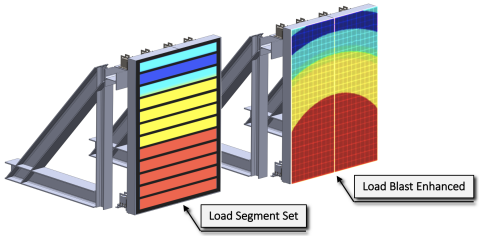

Figure 8: Representation of the different blast effects on the panel, considering LSS and LBE methods in the analysis.

4.4.11 Blast Load Methods

LS-DYNA has four major methods to model blast events, namely Load Blast Enhanced (LBE), Arbitrary Lagrangian-Eulerian (ALE), a hybrid combination of the two methods mentioned (LBE and ALE), and Particle methods. The hybrid and particle methods tend to be used for more complex problems, such as the structural response of a structure, scenarios with multiple wave interactions of multiple explosions, and blast wave reflections with the surrounding environment [43], which in this context did not provide a valid purpose to apply them. Therefore, LBE was the method used.

4.5. Numerical Models

During the numerical study, three types of model geometries have been done. Firstly, the one-quarter of the connector model (initial approach); Secondly the complete connector model (intermediate approach),and finally the complete full model of the system (final approach).

4.6. Calibration and Validation Methods

4.6.1 Blast Load Calibration

Considering the explosive used and its blast characteristics, there are differences compared to its TNT equivalent. It is fairly clear that considering the equivalent charge in TNT, one cannot portray the same effect of the experimental pressure curve, which is descending faster. Blast load calibration is the process of numerically changing TNT mass and distance to achieve the same experimental effects, particularly the same pressure curve slope.

4.6.2 Benchmarking

Through benchmarking, learning the software by practicing with progressively harder examples, which problems and solutions were available, was crucial to virtually understand how to consider blast loads on different constitutive materials or even

variables such as strain-rate, among others necessary aspects.

4.6.3 Mesh Convergence

One issue that is usually overlooked and affects accuracy is mesh convergence or mesh sensitivity study. It is often used in finite element analysis to ensure that computed results converge to the actual solution, whether the problem at hand is linear or nonlinear, that the results are accurate enough, and mesh quality does not significantly influence the final solution [26].

4.6.4 Experimentation

This additional method, consists in the development of the numerical model until its analyses start to produce similar results to the experimental data. In order to represent the correct visual deformation behavior, according to the experimental campaign tests, the entire protective system was modeled. The process intended also, to find the strain-rate parameters that best fit the actual behavior of the system, namely the total inversion. Knowing that in post-processing, it would be possible to replicate the model, it was only built half of the system, precisely a reinforced concrete slab with four EADs.

5. Numerical Analysis

At this point, the 3D model has been created and divided in elements. The model, together with its characteristics have been through calibration methods. Once calibration and validation was achieved, which is a good indication that it is correct, the study was complemented with simulation. Therefore, in this chapter, analysis will be performed, to study solutions and ideas that haven't been tested experimentally. Lastly, conclusions were drawn.

5.1. Simulation 1: Sensitivity analysis of Young Modulus variation

In general, all solid materials are not linear elastic, especially when they are subjected to high levels of deformation. Furthermore blast analysis is highly nonlinear, and this parameter should not have much influence on results. The purpose of this study was to confirm this hypothesis.

As expected, considering all the parameters involved, young's modulus does not influence significantly the performance behavior of the EADs.

5.2. Simulation 2: Hinge ingluence

One interesting feature of this solution is the hinge element, welded in the plate attached to the wall . It was expected that this element would prevent the loss of performance of the system. One must remember that when the system is installed, there is some tendency to have some level of eccentricity as already mentioned. In general, values of total inversion, velocity and internal energy are higher than the compared solution. It additionally reduces the amplification of force on impact.

5.3. Simulation 3: Contact between EAC elements

During the previous analysis, a few aspects stood out. Among them, the risk of contact, between the EAC elements. Therefore, it was analysed the worst case scenario, considering eccentric loading, to accurately assess if there is contact between elements, precisely the inverted tube surface and its adjacent plate edges.

Results data capture the initial bending effect for lower loads, where the tube deforms not only by inversion mechanisms but also by bending mechanism. Being this effect more pronounced for lower loads and having a better efficiency in such scenarios.

5.4. Simulation 4: Deformation behavior

From the results obtained in the previous simulation, some additional findings were made in relation to the development of the EAC deformation mechanisms. Its progression, from bending mechanism transitioning to the buckling mechanism, while simultaneously having inversion deformation mechanism.

An interesting aspect is the angle formed by impactor plate, that receives the hinge on impact, after the blast, which allows to perceive the transition of the different deformation mechanisms.

5.5. Simulation 5: Eccentricity analysis

One of the most relevant analyses is the eccentricity one. An isolated EAD, was analysed under the same loading conditions, corresponding to the experimental load and for 200 kg of TNT, for different eccentricity values.

The total inversion increase, together with internal energy increase as well as higher velocities, can indicate more deformed material, and effortless deformation, therefore more energy-absorption.

It reinforces the resilience of the system, when in a specific case there was contact between elements, and the system instead of worsening, improved its performance by decreasing the peak force (Fig. 9).

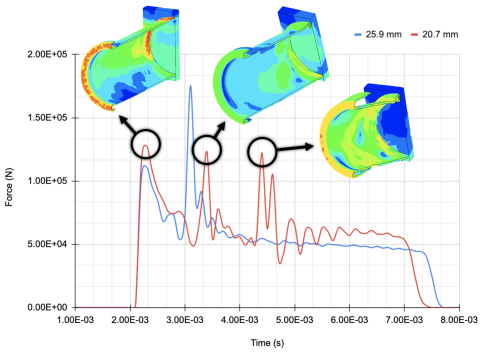

Figure 9: Graph comparing force values for 20.7 [mm] and 25.9 [mm] of eccentricities.

5.6. Simulation 6: Full System Analysis

Considering the deformable and rigid full models of the system, one can observe that internal energy values are higher in the deformable cases.

The capacity of the system is surprisingly good, being virtually able to withstand loads up to 200 kg of TNT, where it has been verified evidence of partial destruction of the wall at the rear side, simultaneously with the exhaustion of the EACs.

6. Conclusions

Taking into account the increasing possibility of terrorist attacks using explosives, it is important to mitigate this threat. In this regard, it is intended to give a contribution by evaluating the performance of this protection system when subjected to the effects of this action. Nonetheless, the present numerical analysis carried out allowed the identification of the most important aspects for the development of a numerical model:

- To model a complex geometry, it is advantageous to consider dedicated third-party software, such as SolidWorks, capable of making the process more practical and less time-consuming;
- Modelling the geometry with full detail can become a waste of time and a waste of resources;
- The integrity of the model, must be confirmed to avoid errors in the analysis;
- To mesh it is beneficial to use third-party software such as HyperMesh, which offers automatic cleaning and meshing functions, saving time and avoiding errors;
- Simplifications, become critical tools to achieve good results in a reasonable time;
- Being a highly dynamic problem, it is vital to consider strain-rate parameters in the model;
- Benchmarking, mesh convergence and experimentation are essential methods to create a trustworthy model;

With regard to the analyses, the most relevant aspects were:

- The numerical analysis confirms the resilience and efficiency of the solution in adverse conditions:
  - When the system has eccentricities;
  - when there is contact between elements;
  - When buckling phenomena occurs;
- EAC deformation limits, are derived from the deformable tube, which can be increased to certain lengths (conditioned by the possibility of global buckling phenomena of the tube);
- The EAC deformation behavior has three states of deformation: i) for lower loads has bending and inversion mechanisms; ii) for higher loads has buckling and inversion mechanisms; in between, it might a joint effect of the three.
- The protective system has the best performance for loads up to 100 kg of TNT. After 200 kg, the EAC exhausts the absorption capacity;
- For severe loads that lead to the exhaustion of the absorption capacity, having the hinge element, significantly reduces the amplification of forces on the protected structure;
- The higher the eccentricity the greater the energy dissipation;
- Bending mechanism leads to a effortless deformation, with less resistance, having a greater energy dissipation, thus reducing peak force values;
- The compounding effect of both bending and inversion deformation mechanisms, improves energy-absorption performance;
- The best results achieved, were obtained with the models where several different plastic deformations have occurred, without the premature rupture of the latter;
- The absorption effect depends not only on the EAC but also on the connector that contains it;

7. Future Work

- Elaboration of a similar analysis with a similar method, tube splitting;
- Elaboration of a similar analysis with the tube filled with energy-dissipation material (e.g., aluminium foam);
- Elaboration of similar analysis of the remaining EADs and its comparison;
- Evaluate the effects of varying geometric properties of the EAC (e.g., diameter and thickness);
- Elaboration of a hybrid analysis, combining different connectors in order to combine their different capacities;
- Analyse the amplification effects of the full entire system;
- Evaluate a mixed solution, which would combine and complement this system;

References

[1] B. J. Buchanan, *Gunpowder, Explosives and the State: A Technological History*, 1st ed. Routledge, 2006. [Online]. Available: https://www.taylorfrancis.com/books/edit/10.4324/9781315253725/gunpowder-explosives-state-brenda-buchanan

[2] M. Vergani, *How Is Terrorism Changing Us?: Threat Perception and Political Attitudes in the Age of Terror*. Palgrave MacMillan, 2018. [Online]. Available: https://www.palgrave.com/gp/book/9789811080654

[3] P. Gill, J. Horgan, and J. Lovelace, "Improvised explosive device: The problem of definition," *Studies in Conflict and Terrorism*, vol. 34, no. 9, pp. 732–748, 2011. [Online]. Available: https://doi.org/10.1080/1057610X.2011.594946

[4] E. Miller, "Trends in Global Terrorism: Islamic State's Decline in Iraq and Expanding Global Impact; Fewer Mass Casualty Attacks in Western Europe; Number of Attacks in the United States Highest since 1980s," START - Study of Terroris and Responses of Terrorism, Tech. Rep. October, 2019. [Online]. Available: https://www.start.umd.edu/pubs/START_GTD_GlobalTerrorismOverview2019_July2020.pdf

[5] D. O. Dusenberry, *Handbook for Blast-Resistant Design of Buildings*. Wiley, Jan 2010. [Online]. Available: https://onlinelibrary.wiley.com/doi/book/10.1002/9780470549070

[6] M. E. Hynes and N. Studies, *Blast Mitigation - Experimental and Numerical Studies*. Springer, Jul 2014. [Online]. Available: https://www.springer.com/gp/book/9781461472667

[7] H. S. Norville, N. Harvill, E. J. Conrath, S. Shariat, and S. Mallonee, "Glass-Related Injuries in Oklahoma City Bombing," *Journal of Performance of Constructed Facilities*, vol. 13, no. 2, pp. 50–56, May 1999. [Online]. Available: https://doi.org/10.1061/(ASCE)0887-3828(1999)13:2(50)

[8] G. Gomes, "Blast Protective Walls Optimization Design (BLADE) - Blast testing report - 10th June's Blast testing on Protective System inversion tubes 64x2mm, NATO Counter IED COE, Madrid Spain." Tech. Rep., 2020.

[9] D. Cormie, G. Mays, and P. Smith, *Blast Effects on Buildings*. London: ICE Publishing, Dec 2019. [Online]. Available: https://www.icebookshop.com/Products/Blast-Effects-on-Buildings,-Third-edition.aspx

[10] K.-U. Schmitt, P. F. Niederer, F. Walz, D. S. Cronin, B. Morrison, and M. H. Muser, *Trauma Biomechanics*, 5th ed. Springer, 2019. [Online]. Available: https://www.springer.com/gp/book/9783030116583

[11] P. W. Cooper, "Comments on TNT equivalence," *20th International Pyrotechnics Seminar*, p. 16, 1994. [Online]. Available: https://www.osti.gov/servlets/purl/10168254

[12] S. D. Adhikary and S. C. Dutta, *Blast resistance and mitigation strategies of structures: Present status and future trends*. ICE Publishing, Apr 2019, vol. 172, ch. 4, pp. 249–266. [Online]. Available: https://www.icevirtuallibrary.com/doi/abs/10.1680/jstbu.17.00056

[13] Gilbert F. Kinney and Kenneth J. Graham, *Explosive Shock in Air*. Springer, 1985. [Online]. Available: https://www.springer.com/gp/book/9783642866845

[14] K. Vasilis and S. George, "Calculation of blast loads for application to structural engineering," European Commission, Luxembourg, Tech. Rep., Dec 2013. [Online]. Available: https://core.ac.uk/download/pdf/38628317.pdf

[15] U. D. U.S. Department of Defense, *UFC 3-340-02*. Department of Defense - United States of America, 2008. [Online]. Available: https://www.wbdg.org/ffc/dod/unified-facilities-criteria-ufc/ufc-3-340-02

[16] W. E. Baker, P. A. Cox, P. S. Westine, J. J. Kulesz, and R. A. Strehlow, *Explosion Hazards And Evaluation*. Elsevier, 1983, vol. 5. [Online]. Available: https://www.elsevier.com/books/explosion-hazards-and-evaluation/baker/978-0-444-42094-7

[17] C. E. Needham, *Blast Waves*. Springer, 2018. [Online]. Available: https://www.springer.com/gp/book/9783319653815

[18] H. L. Brode, "A Calculation of the Blast Wave from a Spherical Charge of TNT, Rand Corp," *Rep. RM-1965 (August 1957)*, p. 61, 1957. [Online]. Available: https://www.rand.org/pubs/research_memoranda/RM1965.html

[19] C. Kingery, G. Bulmash, and U. A. B. R. Laboratory, *Airblast parameters from TNT spherical air burst and hemispherical surface burst*, ser. Technical report ARBRL. US Army Armament and Development Center, Ballistic Research Laboratory, 1984. [Online]. Available: https://books.google.pt/books?id=lg6cHAAACAAJ

[20] R. K. Wharton, S. A. Formby, and R. Merrifield, "Airblast TNT equivalence for a range of commercial blasting explosives," *Journal of Hazardous Materials*, vol. 79, no. 1-2, pp. 31–39, 2000. [Online]. Available: https://pubmed.ncbi.nlm.nih.gov/11040384/

[21] X. Qiu and T. Yu, "Some topics in recent advances and applications of structural impact dynamics," *Applied Mechanics Reviews*, vol. 64, no. 3, 2011. [Online]. Available: https://asmedigitalcollection.asme.org/appliedmechanicsreviews/article-abstract/64/3/030801/370039/Some-Topics-in-Recent-Advances-and-Applications-of

[22] A. Baroutaji, M. Sajjia, and A.-G. Olabi, "On the crashworthiness performance of thin-walled energy absorbers: Recent advances and future developments," *Thin-Walled Structures*, vol. 118, pp. 137–163, 2017. [Online]. Available: https://www.sciencedirect.com/science/article/pii/S0263823116308497

[23] T. S. Pei, S. Nadiah, S. Aishah, and N. Nadiah, "Oblique Impact on Crashworthiness: Review," *International Journal of Engineering Technology and Sciences*, 2017. [Online]. Available: https://journal.ump.edu.my/ijets/article/view/6189

[24] G. Gomes, ""Report of quasi-static inversion tests on thin-walled tubes"," Faculdade de Ciências e Tecnologia da Universidade Nova de Lisboa, Monte da Caparica, Tech. Rep., 2019.

[25] A. Harish, "What is Convergence in Finite Element Analysis?" 2020. [Online]. Available: https://www.simscale.com/blog/2017/01/convergence-finite-element-analysis/

[26] M. Okereke and S. Keates, *Finite Element Applications*. Springer, 2018. [Online]. Available: https://link.springer.com/book/10.1007/978-3-319-67125-3

[27] M. Shuaib and O. Daoud, "Numerical modelling of reinforced concrete slabs under blast loads of close-in detonations using the lagrangian approach," *Journal of Physics: Conference Series*, vol. 628, p. 180, 2015. [Online]. Available: https://www.researchgate.net/publication/280062906_Numerical_Modelling_of_Reinforced_Concrete_Slabs_under_Blast_Loads_of_Close-in_Detonations_Using_the_Lagrangian_Approach

[28] LNLL, "A computer code led to entrepreneurial success," 2014, accessed: 2021-08-03. [Online]. Available: https://www.llnl.gov/news/computer-code-led-entrepreneurial-success

[29] M. Abedini, A. A. Mutalib, C. Zhang, J. Mehrmashhadi, S. N. Raman, R. Alipour, T. Momeni, and M. H. Mussa, "Large deflection behavior effect in reinforced concrete columns exposed to extreme dynamic loads," *Frontiers of Structural and Civil Engineering*, vol. 14, no. 2, pp. 532–553, 2020. [Online]. Available: https://link.springer.com/article/10.1007/s11709-020-0604-9#citeas

[30] Y. Wu, J. E. Crawford, and J. M. Magallanes, "Concrete Constitutive Models," *12th International LS-DYNA Users conference*, no. 1, pp. 1–14, 2012. [Online]. Available: https://www.dynamore.de/de/download/papers/2012-internationale-ls-dyna-users-conference/documents/constitutivemodeling05-a.pdf

[31] C. Wu, J. Li, and Y. Su, *Development of Ultra-High Performance Concrete Against Blasts*. Eslsevier, 2018. [Online]. Available: https://www.elsevier.com/books/development-of-ultra-high-performance-concrete-against-blasts/wu/978-0-08-102495-9

[32] J. W. Wesevich, B. L. Bingham, J. Magnusson, A. P. Christiansen, and D. D. Bogosian, "Comparative Study of Concrete Constitutive Models for Predicting Blast Response," *ACI Symposium Publication*, vol. 281, 2011. [Online]. Available: https://www.concrete.org/publications/internationalconcreteabstractsportal/m/details/id/51683609

[33] S. H. Yang, K. S. Woo, J. J. Kim, and J. S. Ahn, "Finite Element Analysis of RC Beams by the Discrete Model and CBIS Model Using LS-DYNA," *Advances in Civil Engineering*, vol. 2021, 2021. [Online]. Available: https://www.hindawi.com/journals/ace/2021/8857491/

[34] Y. D. Murray, A. Abu-Odeh, and R. Bligh, "Evaluation of LS-DYNA Concrete Material Model 159," *Report No. FHWA-HRT-05-063*, no. May, p. 209, 2007. [Online]. Available: https://www.fhwa.dot.gov/publications/research/infrastructure/structures/05063/index.cfm

[35] J. Hallquist, *LS-DYNA Keyword User's Manual I*. Livermore Software Technology Corportation (LSTC), 2007, vol. I, no. February. [Online]. Available: https://lstc.com/pdf/ls-dyna_971_manual_k.pdf

[36] G. R. Cowper and P. S. Symonds, "Strain-hardening and strain-rate effects in the impact loading of cantilever beams," 1957. [Online]. Available: https://apps.dtic.mil/sti/pdfs/AD0144762.pdf

[37] "Dynamic axial crushing of circular tubes," *International Journal of Impact Engineering*, vol. 2, no. 3, pp. 263–281, 1984. [Online]. Available: https://www.sciencedirect.com/science/article/pii/0734743X84900101

[38] W. Abramowicz and N. Jones, "Dynamic progressive buckling of circular and square tubes," *International Journal of Impact Engineering*, vol. 4, no. 4, pp. 243–270, 1986. [Online]. Available: https://www.sciencedirect.com/science/article/pii/0734743X86900175

[39] Y. Jilin and J. Norman, "Further experimental investigations on the failure of clamped beams under impact loads," *International Journal of Solids and Structures*, vol. 27, no. 9, pp. 1113–1137, 1991. [Online]. Available: https://www.sciencedirect.com/science/article/pii/002076839190114U

[40] S. Marais, R. Tait, T. Cloete, and G. Nurick, "Material testing at high strain rate using the split hopkinson pressure bar," *Latin American Journal of Solids and Structures*, vol. 1, p. 20, 06 2004. [Online]. Available: https://www.lajss.org/index.php/LAJSS/article/download/53/47/50

[41] H. Jama, M. Bambach, G. Nurick, R. Grzebieta, and X.-L. Zhao, "Numerical modelling of square tubular steel beams subjected to transverse blast loads," *Thin-Walled Structures*, vol. 47, pp. 1523–1534, 12 2009. [Online]. Available: https://www.researchgate.net/publication/223785563_Numerical_modelling_of_square_tubular_steel_beams_subjected_to_transverse_blast_loads

[42] M. Sun and J. Packer, "High strain rate behaviour of cold-formed rectangular hollow sections," *Engineering Structures*, vol. 62–63, p. 181–192, 03 2014. [Online]. Available: https://www.researchgate.net/publication/260231369_High_strain_rate_behaviour_of_cold-formed_rectangular_hollow_sections/citations

[43] J. Trajkovski, "Comparison of MM-ALE and SPH methods for modelling blast wave reflections of flat and shaped surfaces," *11th European LS-DYNA User Conference, Salzburg, Austria*, no. May 2017, p. 15, 2017. [Online]. Available: https://www.researchgate.net/publication/317560674_Comparison_of_MM-ALE_and_SPH_methods_for_modelling_blast_wave_reflections_of_flat_and_shaped_surfaces